Phase-Dependent Resistance in a Superconductor–Two-Dimensional-Electron-Gas Quasiparticle Interferometer

A. Dimoulas, J. P. Heida, B. J. v. Wees, and T. M. Klapwijk
Department of Applied Physics and Materials Science Center, University of Groningen, Nijenborgh 4, 9747 AG Groningen, The Netherlands

W. v. d. Graaf and G. Borghs
Interuniversity Microelectronics Center, Kapeldreef 75, B-3030, Leuven, Belgium
(Received 15 June 1994)

We have investigated the interplay between Josephson coupling and quasiparticle interference effects in the resistance of a two-dimensional electron gas connected to superconducting electrodes with an interrupted ring geometry. By reducing the influence of the Josephson coupling strength at high dc current bias and large interelectrode spacing, we observed magneto-oscillations in the resistance with a period $h/2e$, which we attribute to quasiparticle interference.

PACS numbers: 74.50.+r, 85.25.Dq, 85.25.Jw

The phase of the order parameter of a superconductor plays a crucial role in the supercurrent flow in bulk superconductors as well as in Josephson junctions and weak links. It has been predicted [1] that the *resistance* of a piece of normal metal or semiconductor connected to two superconductors can also depend on the superconducting phase difference established between them. We can exploit this property to study quasiparticle interference effects at the superconductor-normal interface. The basic idea is that, if the superconducting phase difference is externally controlled between 0 and π, the resistance of the normal layer could be influenced, alternately, by constructive and destructive interference of quasiparticles.

A quasiparticle interferometer has been proposed [2] in which the superconducting phase difference could be controlled by a supercurrent passing through a Josephson junction. Other interferometer structures have been studied theoretically [3–5]. Experimental work on a normal metal superconducting quantum interference device, based on the modulation of Andreev conductance, has recently been reported [6,7]. The latter device operates in the limit of low mobility diffusive transport in the normal layer and very low transparency at the interface, appropriate to tunnel junctions. Under these conditions, the experimental results [6] can be understood reasonably well by the existing theory [3,4] for phase coherent Andreev reflection [8–11]. However, in the case of (quasi)ballistic transport and near unity interface transparency, theoretical and experimental progress is not sufficient at the present time for the understanding of quasiparticle transport. A number of experiments have been reported on supercurrent transport in Josephson-type junctions using the Nb/InAs system with a highly transmissive interface [12,13]. Quasiparticle interferometer structures in this regime have not been investigated experimentally.

In this Letter, we have realized a quasiparticle interferometer, made of Nb electrodes on top of a high mobility InAs two-dimensional-electron-gas layer, which operated in the limit of quasiballistic transport and high transparency at the interfaces. The superconducting phase difference was controlled by a magnetic field, through a ring-shaped Nb electrode. Because of the transparent interfaces, we expected to observe both quasiparticle interference as well as Josephson coupling between the electrodes. We were able to distinguish between the two effects and, either at high dc biases or at large interelectrode spacing, we obtained clear evidence for quasiparticle interference which we studied as a function of dc voltage bias and temperature.

The semiconductor structures were grown on a GaAs substrate and had the form of a quantum well: 2 μm GaSb buffer layer (barrier)/20 nm InAs active layer (well)/20 nm GaSb top layer (barrier). The InAs well carried a degenerate two-dimensional electron gas with $n_s = 9.0 \times 10^{11}$ cm^{-2}. The electron mobility at 4.2 K was found to be $\mu_e \simeq 48\,000$ V cm^2/sec, implying a mean free path $l \simeq 0.75$ μm. The superconductor electrodes were fabricated by standard electron beam lithography and lift-off techniques. Prior to deposition of 70 nm of Nb superconductor, the top GaSb layer was wet etched and the free surface of InAs was ion cleaned under vacuum. We have chosen InAs because the absence of a Schottky barrier in this material results in a transparent semiconductor-superconductor interface [12]. Our measurements [13] on single junctions processed on the same chip indicated clean interfaces with a high transmission probability $T \sim 0.8$. The measuring ac excitation current depended on the experimental conditions and, in any case, it was kept smaller than the estimated critical current, while the corresponding ac voltage was smaller or comparable to k_BT/e.

The general characteristic of the devices, shown in Fig. 1(a), is that one of the superconducting electrodes (electrode 1) has a ring-shaped geometry, with an inter-

 0031-9007/95/74(4)/602(4)$06.00

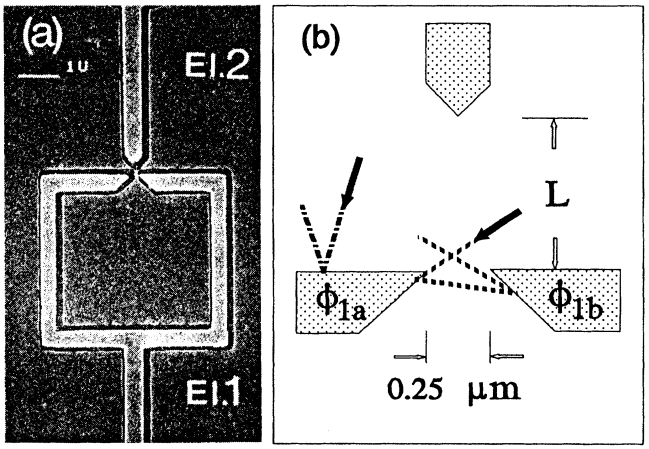

FIG. 1. Layout of the interferometer made of planar superconducting Nb electrodes on the top of an InAs 2DEG. (a) SEM picture showing electrode 2 (El.2) and the ring-shaped electrode 1 (El.1). (b) A schematic drawing which shows in detail electrode 2 and the two arms 1a and 1b of electrode 1, with superconducting phases ϕ_{1a} and ϕ_{1b}, respectively. The interelectrode spacing L was 0.3, 1, and 2 μm. The dotted and dash-dotted lines show two typical trajectories for quasiparticles.

ruption of 0.25 μm at one side. From measurements on single junctions with a similar geometry [13] we expect that Josephson coupling is present between the two arms 1a and 1b of the ring electrode [Fig. 1(b)]. However, this Josephson coupling will not affect our measurements since both arms are at the same potential. Because of the fact that all electrodes are made of Nb, Josephson coupling is also expected between electrode 2 and 1a as well as between electrode 2 and 1b. Therefore, in first order, the device is similar to a dc superconducting quantum interference device (SQUID). To investigate the influence of different Josephson coupling strength between electrodes 1 and 2, we placed electrode 2 at several distances $L = 0.3$, 1.0, and 2.0 μm away from the interruption in the ring [Fig. 1(b)]. This allowed us to distinguish between the Josephson and quasiparticle interference effects. Because of the ring-shaped geometry of electrode 1, the superconducting phase difference $\phi = \phi_{1a} - \phi_{1b}$ between the two arms of the ring can be controlled by an externally applied magnetic field according to $\phi = 2\pi(\Phi/\Phi_0)$, where Φ is the magnetic flux penetrating the ring area and Φ_0 is the superconducting magnetic flux quantum $h/2e$. Quasiparticles in the semiconductor undergo Andreev reflection at the interface with the superconductor which implies a phase shift by an amount proportional to the superconducting phase. Therefore, Andreev-reflected quasiparticles following a path [dotted line in Fig. 1(b)] at the vicinity of the ring interruption are influenced by both arms and can produce a ϕ-dependent interference term in the resistance (conductance) of the semiconductor between electrodes 1 and 2. There is also a constant contribution from carriers which sense only one of the two arms [path denoted by the dash-dotted line in Fig. 1(b)], so that the total differential conductance measured at a dc voltage V and temperature T will be modulated by the magnetic flux according to the phenomenological expression

$$G(V,T) = G_{1a} + G_{1b} + \Delta G(V,T)\cos(2\pi\Phi/\Phi_0). \quad (1)$$

Here, $\Delta G(V,T)$ is the amplitude of the quasiparticle interference term and G_{1a} and G_{1b} are the contributions from carrier transport between electrode 2 and arms 1a and 1b, respectively. In the absence of a detailed microscopic theory applicable to our case (two-dimensional geometry and high transparency interfaces), expression (1) is considered only as a guideline to appreciate the role of the magnetic flux in modulating the conductance.

In the experiment we measured the differential resistance between electrodes 1 and 2, as a function of the magnetic field B, for different dc current biases I_{dc}. A typical set of data obtained at 100 mK and zero I_{dc} is shown in Fig. 2. The main observation is a large number of oscillations in the resistance with a period of about 1 G, which are clearly resolved in the samples with $L = 0.3$ and 1.0 μm. The period corresponds to the value of B at which the flux through the area $A \simeq 20\,\mu\text{m}^2$ of the ring changes by, approximately, Φ_0. In the case of the $L = 0.3$ μm sample, the resistance becomes zero for values of B less than 10 G. For this range of the magnetic field, a supercurrent was observed (not shown), oscillating with the same period between a maximum value of 400 nA and a minimum of about zero. This shows that the device behaves similar to a SQUID consisting of two Josephson junctions formed between electrode 2 and each one of the two arms 1a and 1b of the ring electrode. This description is further supported by the dependence of the magnitude of the oscillations on the interelectrode spacing. As L increased to 1.0 μm, the Josephson coupling weakened and

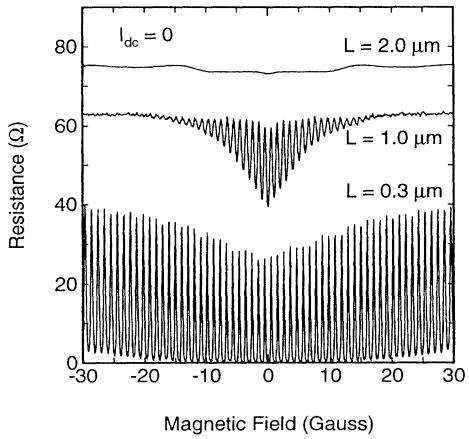

FIG. 2. Differential resistance vs magnetic field, illustrating Josephson-type oscillations at zero dc current bias I_{dc} and $T = 100$ mK. L is the interelectrode spacing.

a finite resistance developed as a result of thermal fluctuations [14]. This resistance was modulated with a maximum change of ~40%, indicative of a value of the critical current I_c about 50 nA. For a larger spacing of $L = 2.0$ μm, the Josephson coupling strength dropped dramatically, as seen from Fig. 2. In a magnified scale, small amplitude oscillations can still be resolved in the $L = 2.0$ μm spectrum, which, however, are *not* Josephson oscillations, as will be discussed below.

As an alternative way to reduce the influence of the Josephson coupling strength, we increased I_{dc} above 5.0 μA, which is at least an order of magnitude higher than I_c, a level at which the Josephson effect is expected to be dramatically reduced. We observed a different set of oscillations of much smaller amplitude, but approximately the same period $h/2e$, in all three types of devices. A typical set of spectra obtained at $I_{dc} = 5$ μA and a temperature of 100 mK is shown in Fig. 3(a). The low and high bias oscillations for the $L = 1.0$ μm sample are plotted together in Fig. 3(b) for comparison. It is claimed here that the high bias oscillations shown in Figs. 3(a) and 3(b) (solid curves) are due to quasiparticle

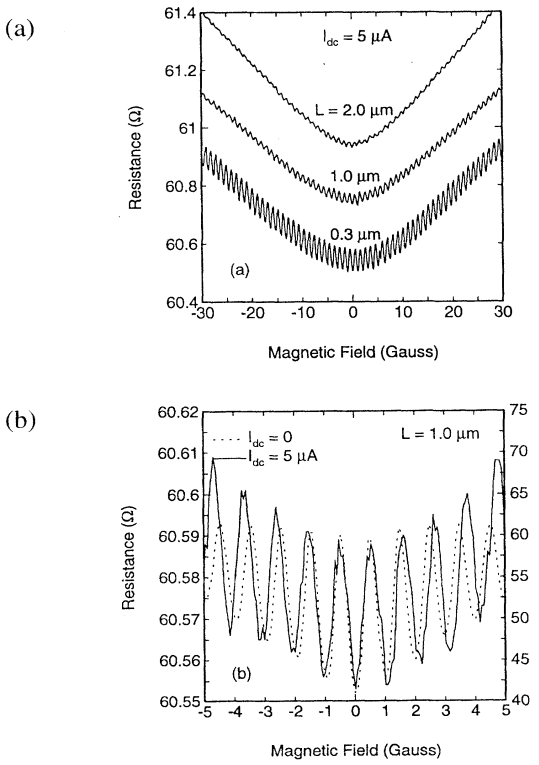

FIG. 3. (a) Oscillations in the differential resistance due to quasiparticle interference at high dc current bias I_{dc}. The spectra of the $L = 0.3$ and 2.0 μm samples were given an offset of +10 and −14 Ω, respectively. (b) The oscillations at high (−) and low (- -) dc current bias (plotted together on the same graph for comparison) correspond to the scale on the left and the right axis, respectively. All spectra were obtained at $T = 100$ mK. L is the interelectrode spacing.

interference and can be clearly distinguished from the Josephson-type ones appearing at low bias, because they exhibit distinctly different characteristics: First, the high bias oscillations showed only a very small sensitivity to the interelectrode spacing [Fig. 3(a)] and they were clearly resolved even in the $L = 2.0$ μm sample, for which no Josephson-type oscillations were observed at low bias (Fig. 2). The amplitude near zero magnetic field decreased from 0.07 to 0.02 Ω, when L increased from 0.3 to 2 μm. This is because fewer electrons sense both arms of the ring as the electrode 2 is pulled farther apart, and the contribution to the quasiparticle interference decreases. Second, we note that the period $\Delta B \simeq 1.03$ G of the high bias oscillations is slightly larger compared to the one at low bias, as seen from Fig. 3(b). This period corresponds to an area $\Phi_0/\Delta B$, which is equal, within the experimental error, to the area of the ring itself. This indicates that the effect is localized to a small region near or within the ring interruption, which is expected for quasiparticle interference. To appreciate the importance of this observation, we make the comparison with the low bias oscillations. These oscillations have a smaller period by 0.025 G [Fig. 3(b)], which implies that the effective area associated with the SQUID behavior is enlarged relative to the area of the ring by ~0.5 μm^2. The latter corresponds, approximately, to the semiconductor area defined by the two arms of the ring and electrode 2, consistent with the description in terms of Josephson coupling between electrodes. It is also seen from Fig. 3(b) that both types of oscillations exhibit a minimum at $\Phi = n\Phi_0$. This property provides further evidence that the high bias oscillations are not related to a dc SQUID behavior, since, in such a case, a maximum in the differential resistance would be expected [14] for $I_{dc} \gg I_c$. Finally, we clearly see from Fig. 3(a) that the amplitude of the high bias oscillations varies very slowly with B, which, in the case of the $L = 1.0$ μm sample, is in contrast to the rapid decrease of the Josephson-type ones in Fig. 2. Indeed, the latter disappear around 20 G, which is expected under the assumption that approximately one flux quantum penetrating the area between the electrodes quenches the Josephson coupling. On the contrary, at high bias [Fig. 3(a)], the amplitude is reduced only by a small fraction when B is increased from 0 to 30 G and the oscillations remain resolved up to 100 G. This is again consistent with the fact that the effect takes place near or between the arms of the ring.

In order to investigate the quasiparticle interference in more detail, we present in Fig. 4 the amplitude of the oscillations, expressed in terms of differential conductance changes ΔG, as a function of the dc voltage bias for the $L = 2.0$ μm sample. Positive (negative) ΔG amplitudes mean that the conductance has a maximum (minimum) at $B = 0$ or at any other value of B for which $\Phi = n\Phi_0$. Remarkably, the effect persists to high voltages (up to 1.3 mV), although the effective energy of electrons which contributes to the interference may be only a fraction of

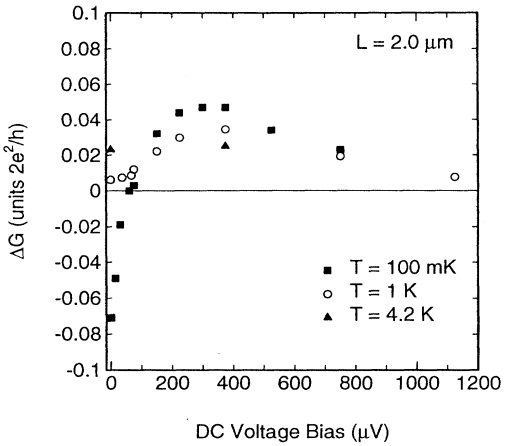

FIG. 4. The amplitude of the interference oscillations expressed in terms of conductance changes ΔG, plotted as a function of dc voltage bias, for three different temperatures.

the dc voltage across the device. It is also interesting to observe that, in the low temperature case of $T = 100$ mK (filled squares), there is a crossover at about 50 μV, between negative and positive values of ΔG. The negative sign around zero bias excludes the possibility that these are Josephson oscillations. Also, apart from the difference in sign, all other characteristics such as the period and the variation of their amplitude with B are the same, indicating that the oscillations have their origin in quasiparticle interference over the whole range of voltages. This in turn implies that the latter oscillations are most probably present in the samples with $L = 0.3$ and 1.0 μm also at low biases, although they cannot be resolved in Fig. 2 since they are masked by the much stronger Josephson effect.

The behavior in response to a temperature and a voltage increase, presented in Fig. 4, can be described consistently in terms of energy averaging [15]:

$$\Delta G(V,T) = \int_{-\infty}^{\infty} [-df(E - eV)/dE] \Delta G(E) dE . \quad (2)$$

Here, $\Delta G(E)$ describes the contribution to the interference amplitude of electrons at energy E. Because of thermal smearing of the Fermi-Dirac distribution f, the contribution from higher energies increases as we raise the temperature, which may explain the positive sign of ΔG above 1 K, over the whole range of voltages.

The crossover between negative and positive values of ΔG in the 100 mK curve is not yet understood. Several authors [2,3,5] have predicted a *maximum* in the conductance at $\Phi = n\Phi_0$, in various interferometer structures. However, these theories do not apply to the multichannel, quasiballistic case with highly transmissive interfaces. Recent calculations in interferometer structures [4] predict a *minimum* in the conductance at $\Phi = n\Phi_0$, in the limit of high barrier transparencies and at low temperatures and voltages. However, it is unclear whether this theory can be directly applied to our measurements because of the two-dimensional geometry of our devices. It is worth mentioning that, in the case of transparent interfaces, a negative ΔG value at $\Phi = n\Phi_0$ may also arise from (enhanced) weak localization [10,11,16] due to phase-coherent Andreev reflection. Note, however, that if such an effect were important in our case, it would have resulted in $h/4e$ periodicity [1,16], which was not observed within the detection limit of our measurement ($\Delta R = 5$ mΩ).

In conclusion, we have shown that the conductance of a two-dimensional electron gas connected to two superconductors is modulated by the superconducting phase difference. The details of the behavior with voltage and temperature may provide information about the physical processes affecting quasiparticle transport at the semiconductor-superconductor interface.

This work was supported by the Netherlands Organization for Scientific Research (NWO) through the Foundation for Fundamental Research on Matter (FOM). A. D. acknowledges support from the European Human Capital & Mobility Programme and B. J. v. W. from the Dutch Royal Academy of Sciences.

[1] B. Z. Spivak and D. E. Khmel'nitskii, JETP Lett. **35**, 412 (1982); B. L. Al'tshuler and B. Z. Spivak, Sov. Phys. JETP **65**, 343 (1987).
[2] H. Nakano and H. Takayanagi, Phys. Rev. B **47**, 7986 (1993).
[3] F. W. J. Hekking and Yu. V. Nazarov, Phys. Rev. Lett. **71**, 1625 (1993); Y. V. Nazarov (to be published).
[4] A. V. Zaitsev (to be published).
[5] C. J. Lambert, J. Phys. Condens. Matter **5**, 707 (1993).
[6] H. Pothier, S. Guéron, D. Esteve, and M. H. Devoret (to be published).
[7] The influence of superconducting contacts on the Aharonov-Bohm effect has been investigated by V. T. Petrashov, V. N. Antonov, P. Delsing, and T. Claeson, Phys. Rev. Lett. **70**, 347 (1993).
[8] B. J. van Wees, P. de Vries, P. Magnée, and T. M. Klapwijk, Phys. Rev. Lett. **69**, 510 (1992).
[9] A. V. Zaitsev, JETP Lett. **51**, 41 (1990); A. F. Volkov, A. V. Zaitsev, and T. M. Klapwijk, Physica (Amsterdam) **210C**, 21 (1993).
[10] C. W. J. Beenakker, Phys. Rev. B **46**, 12 841 (1992); I. K. Marmorkos, C. W. J. Beenakker, and R. A. Jalabert, Phys. Rev. B **48**, 2811 (1993).
[11] Y. Takane and H. Ebisawa, J. Phys. Soc. Jpn. **61**, 3466 (1992).
[12] J. Nitta, T. Akazaki, H. Takayanagi, and K. Arai, Phys. Rev. B **46**, 14 286 (1992); C. Nguyen, H. Kroemer, and E. L. Hu, Phys. Rev. Lett. **69**, 2847 (1992).
[13] J. P. Heida, A. Dimoulas, F. van Looyengoed, B. J. van Wees, T. M. Klapwijk, and G. Borghs (unpublished).
[14] V. Ambegaokar and B. I. Halperin, Phys. Rev. Lett. **22**, 1364 (1969).
[15] See, for example, C. W. J. Beenakker and H. van Houten, Solid State Phys. **44**, 1 (1991).
[16] Y. Takane and H. Otani (to be published).

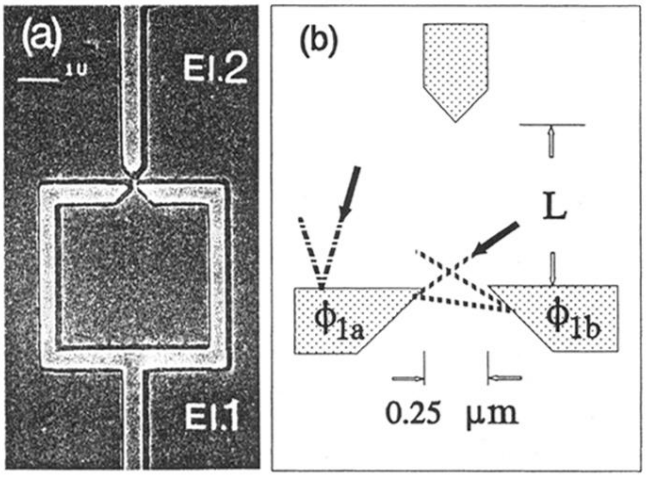

FIG. 1. Layout of the interferometer made of planar superconducting Nb electrodes on the top of an InAs 2DEG. (a) SEM picture showing electrode 2 (El.2) and the ring-shaped electrode 1 (El.1). (b) A schematic drawing which shows in detail electrode 2 and the two arms 1a and 1b of electrode 1, with superconducting phases ϕ_{1a} and ϕ_{1b}, respectively. The interelectrode spacing L was 0.3, 1, and 2 μm. The dotted and dash-dotted lines show two typical trajectories for quasiparticles.